IOP Conf. Series: Journal of Physics: Conf. Series **1256** (2019) 012023 doi:10.1088/1742-6596/1256/1/012023

Effects of Inflow Spatiotemporal Discretization on Wake Meandering and Turbine Structural Response Using FAST.Farm

K. Shaler, J. Jonkman, and N. Hamilton

National Renewable Energy Laboratory, Golden, CO 80401, USA

E-mail: kelsey.shaler@nrel.gov

Abstract. FAST.Farm is a newly developed multiphysics, midfidelity engineering tool that can be used to predict turbine power and structural loads of wind turbines in a wind farm with minimal computational expense. Previous studies have shown similarities and differences in wind turbine performance between FAST.Farm and high-fidelity large-eddy simulations (LES) using both LES precursor-generated inflow and TurbSim-generated synthetic inflow. While conservative resolutions have been used to date, no formal spatial or temporal discretization study has been performed for the FAST.Farm model wind domains. This work aims to study the effects of varying the spatial and temporal discretization of the wind domains on wake meandering (low-resolution domain) and turbine structural response (high-resolution domains) and resulting wake and load calculations. The purpose of this study is to establish convergence criteria and recommendations for discretization values in terms of rotor diameter (D, expressed in meters) that will maximize computational efficiency. To ensure a percent error of $\leq 1\%$ in standard deviation of wake center position relative to the finest included resolution, a low-resolution time step of $0.024D$ s, $0.016D$ s, and $0.0079D$ s and a low-resolution spatial discretization of $0.079D$ m, $0.16D$ m, and $0.24D$ m is recommended for 8 m/s, 12 m/s, and 18 m/s mean ambient wind speed at hub height, respectively. These guidelines are likely applicable to other implementations of the dynamic wake meandering model. To ensure a percent error of $\leq 1\%$ in standard deviation of all considered structural response outputs, a high-resolution time step that captures the highest influential excitation and natural frequencies in the system and a high-resolution spatial discretization comparable to the maximum airfoil cord length is recommended. These guidelines are likely applicable to any aeroelastic analysis.

1. Introduction

In the context of wind farm design and optimization, it is crucial to be able to perform thousands of wind farm-scale simulations in near-real time. FAST.Farm is a new midfidelity tool developed by the National Renewable Energy Laboratory (NREL) for this purpose. As an extension of the widely used OpenFAST code, it aims to model the wake physics of wind farms for the purpose of accurately and efficiently predicting power production and structural loading of each wind turbine in the farm. In past work, FAST.Farm input parameters were calibrated against high-fidelity large-eddy simulations (LES) implemented in the Simulator fOr Wind Farm Applications (SOWFA) [2] and later verified against SOWFA simulations [6, 9] for different inflow and

operation conditions when using ambient wind data generated by both LES-precursor-generated inflow and TurbSim-generated synthetic inflow. The verification study showed that FAST.Farm did reasonably well at capturing the statistical distributions of generator power, torque, rotor thrust, and rotor speed for single- and three-turbine configurations. Additionally, horizontal and vertical wake meandering as well as wake-deficit advection, evolution, and merging were predicted reasonably well by FAST.Farm for most cases. While these results are promising, conservative resolutions have been used to date and no formal spatial or temporal discretization study has been performed for the wind domains of the FAST.Farm model.

This work aims to quantify the effects of varying the spatial and temporal discretization in FAST.Farm simulations for both the low-resolution wind domain used for wake meandering, and the high-resolution wind domains used for turbine structural response and load calculations. The purpose of these studies is to determine resolution requirements to achieve solution convergence and establish recommended discretization values for FAST.Farm users that will maximize computational efficiency. While FAST.Farm is the focus, the results are likely applicable to other aeroelastic and dynamic wake meandering models.

2. Approach and Methods

This section provides an overview of FAST.Farm, followed by descriptions of the modeling cases that were used in this study.

2.1. Overview of FAST.Farm

FAST.Farm is a multiphysics engineering tool that accounts for wake interaction effects on turbine performance and structural loading within wind farms. FAST.Farm is an extension of the NREL software OpenFAST, which solves the aero-hydro-servo-elasto dynamics of individual turbines. FAST.Farm extends this analysis to include wake deficits, advection, deflection, meandering, and merging for wind farms. FAST.Farm is based on the dynamic wake meandering (DWM) model [8], but expands on it to address many limitations of past DWM implementations. Using this method, the wake deficit of each turbine is computed using the steady-state thin shear layer approximation of the Navier-Stokes equations and the wake is perturbed with a turbulent freestream to capture wake meandering. Wake merging is modeled using a superposition method. As in OpenFAST, rotor aerodynamics are modeled using the blade-element momentum (BEM) theory with options for advanced corrections, including unsteady aerodynamics. The FAST.Farm implementation of DWM is an enhancement over past implementations primarily because of the:

(i) Optional use of LES-generated precursors for ambient wind
(ii) Improvement of wake advection, deflection, and merging
(iii) Optional inclusion of a wind farm-wide super controller
(iv) Ability to solve the entire wind farm using parallelization of the computations, and
(v) Calibration of wake-related model parameters against SOWFA simulations.

A complete description of the FAST.Farm theory and implementation is available in [4] and [7].

2.2. Modeling Cases

The FAST.Farm inflow is composed of a single low-resolution domain throughout the wind farm and smaller, high-resolution domains surrounding each turbine. Each domain has an associated spatial (dS) and temporal (dT) discretization of the inflow, as described further in [7]. These discretization levels are independent of other spatial and time steps associated with the simulations. Herein, spatial and temporal discretization studies were performed for the low- and high-resolution inflow domains. The studies were performed for one domain while holding

discretization of the other domain constant, which is possible due to their relative independence. In previous studies, [2, 6, 9] which involved analysis of single- and three-turbine configurations of the NREL 5-MW reference turbine [5] with ambient wind speeds of 8 m/s at hub height, the low-resolution domain had a spatial resolution (dS_{Low}) of 10 m and a temporal resolution (dT_{Low}) of 2 s, whereas the high-resolution domains had a spatial resolution (dS_{High}) of 10 m and a temporal resolution (dT_{High}) of 0.333 s. This dT_{High} value was expected to be sufficient for capturing turbine thrust and power but not structural loading in general. These values were used as a starting point in the present study, with minor differences as described in the following section. The wake discretization in FAST.Farm (not discussed further in this work) consists of 140 wake planes released parallel to each rotor, each with a radial finite-difference grid of 40 radial nodes.

In this paper, discretization studies were performed for a row of three aligned NREL 5-MW reference turbines (rotor diameter of $D = 126$ m) for low (6%) and high (10%) turbulence intensity (TI). For each level of TI, three wind speeds were considered, representing below-, near-, and above-rated wind speeds – 8 m/s, 12 m/s, and 18 m/s at hub height, respectively. Turbulent wind conditions were generated using TurbSim [3] for each of the six combinations of wind speed and TI. Turbulence was generated using the Kaimal spectrum and exponential coherence model–based on the specified TI and shear exponent–in accordance with International Electrotechnical Commission (IEC) guidelines [1]. All pertinent structural degrees of freedom (blade, drivetrain, tower) and the turbine control system are enabled in each OpenFAST wind turbine model. For the low-resolution discretization study, a single 1-hour simulation was performed for each case using one turbulent inflow realization for each wind condition. For the high-resolution discretization study, six 10-minute simulations were performed for each case using six different turbulent inflow realizations at each wind condition. This was done because the required computational time to generate a 1-hour turbulent inflow file with a fine spatial discretization over a large domain is significant. Instead, six 10-minute inflow files can be generated in parallel, significantly reducing inflow file generation time. When six 10-minute simulations were run, the time-series results were concatenated into a single 1-hour result for post-processing. Start-up transients were removed from the analysis by neglecting the first 300 seconds of each simulation before processing output. For each turbulence intensity and wind speed, spatial and temporal discretization were studied. The discretization cases are summarized in Table 1.

Table 1. Spatial and temporal discretization ranges considered for each of the six atmospheric inflow conditions.

Domain	**Spatial Discretization**	**Temporal Discretization**
Low-Res.	$dS_{Low} = 5$ m – 30 m	$dT_{Low} = 0.333$ s – 10 s
High-Res.	$dS_{High} = 5$ m – 30 m	$dT_{High} = 0.05$ s – 0.5 s

The lower limits of the spatial and temporal resolutions for the high-resolution discretization study were chosen based on turbulence modeling rules of thumb for wind turbine aeroelastic simulations, i.e., using a spatial step based on the maximum chord length (approximately 5 m for the NREL 5-MW turbine) and a time step that captures the frequency range of turbulence that may impact turbine structural response (about 10 Hz, or time step of 0.05 s based on the Nyquist frequency), respectively. The spatial and temporal resolutions were arbitrarily increased in steps of 5 m and ~ 0.1 s above these lower limits. To accommodate the lower frequency range pertinent to wake meandering, the temporal resolution lower limit was increased to 0.333 s

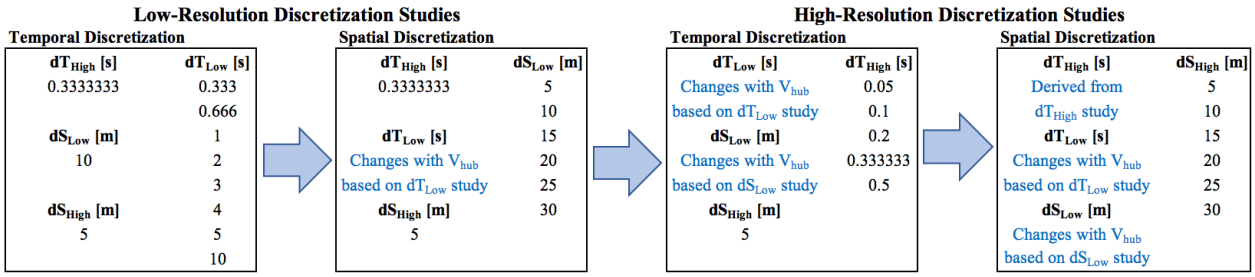

Figure 1. Flowchart of discretization study sequence.

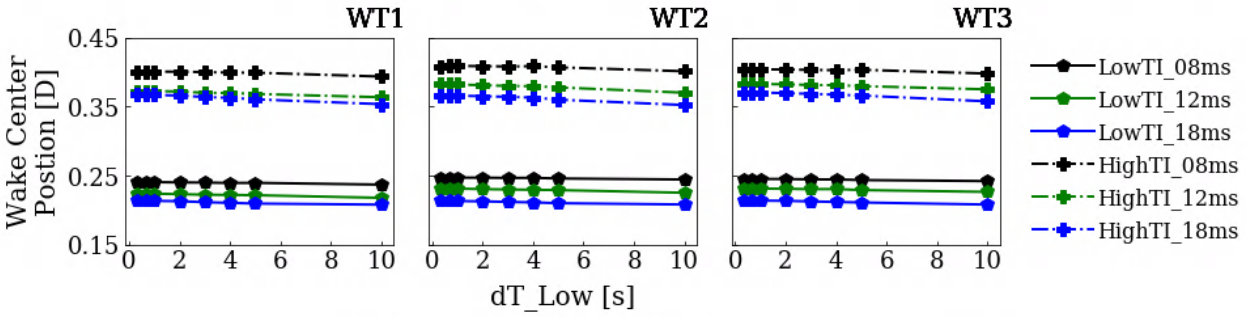

Figure 2. Standard deviation of lateral wake center position associated with each dT_{Low} value at 8D downstream of each turbine.

and the step sizes were changed as well. Temporal and spatial discretizations were varied independently while holding the other quantities fixed. First, the required temporal and spatial discretizations to accurately capture wake meandering-related quantities were determined. For this step, the high-resolution discretization levels were fixed at 5 m and 0.333 seconds. Based on these results, the required high-resolution discretizations to accurately capture turbine structural response were determined. This process is summarized in Figure 1.

3. Results

3.1. Low-Resolution Discretization Study

The low-resolution domain is primarily responsible for wake meandering and merging and so this was the focus of the first level of analysis. Specifically, convergence was assessed by comparing trends in standard deviation of lateral and vertical meandering wake center positions for the wakes behind each turbine at various distances downstream. For all quantities in each case, the percent error was computed relative to the lowest discretization values considered – $dT_{Low} = 0.333$ s and $dS_{Low} = 5$ m. During the initial assessment of convergence, mean lateral and vertical wake center positions were also considered. For both quantities, minimal changes were shown for varying dT_{Low} and dS_{Low}, with percent errors of mean vertical wake center position remaining within 1% for all considered values. Because the mean wake position showed no sensitivity to the discretization, convergence was assessed based only on standard deviations of the meandering wake center position.

3.1.1. Temporal Discretization The variation of lateral meandering wake center position standard deviation for various dT_{Low} values 8D downstream of each turbine is shown in Figure 2. Results are grouped by turbulence intensity and, as expected, have higher standard deviation for inflow with higher TI. For a given TI level, higher mean wind speeds result in lower wake

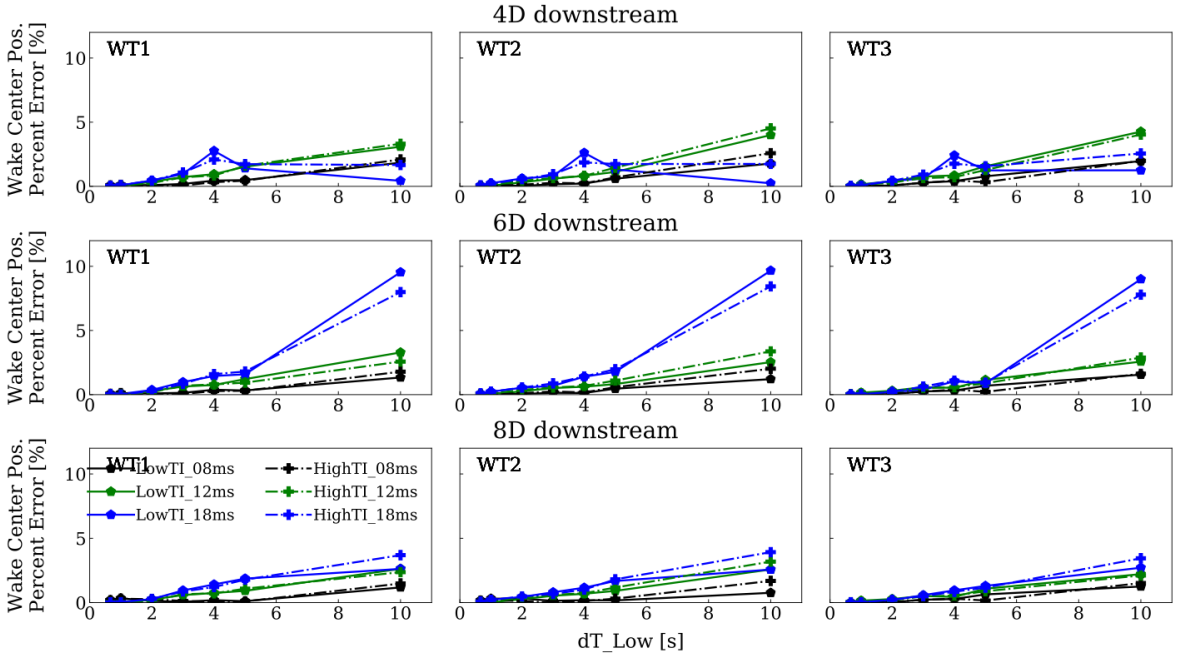

Figure 3. Percent error of lateral wake center position standard deviation associated with each dT_{Low} value for several distances downstream of each turbine.

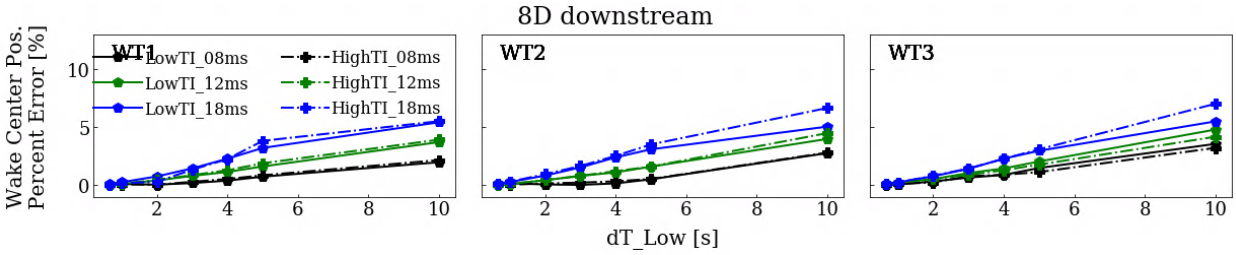

Figure 4. Percent error of vertical wake center position standard deviation associated with each dT_{Low} value at 8D downstream of each turbine.

meandering because it takes less time for a wake to propagate to 8D downstream of each turbine. Trends shown here are representative of standard deviations for both lateral and vertical wake position. To more clearly highlight differences due to varying dT_{Low}, percent error relative to $dT_{Low} = 0.333$ s is computed and shown for lateral wake meandering in Figure 3 for multiple downstream distances. Though percent errors reach up to $\sim$ 12% for $dT_{Low} = 10$ s at 2D downstream, this is largely due to the small value used for the "truth" solution. Overall, percent error converges to a low value for decreasing dT_{Low}. In general, values are grouped by mean ambient wind speed and are independent of turbulence intensity. Similarly, convergence plots of dT_{Low} for standard deviation of vertical wake position at a single downstream distance are shown in Figure 4. From these results, the maximum dT_{Low} value required for a desired percent error bound was selected for each inflow condition, considering each turbine and downstream distance. These required values are shown in Figure 5. For this work, a percent error bound of 1% was chosen. Thus, for the subsequent discretization studies, dT_{Low} values are selected to be 3, 2, and 1 s for 8, 12, and 18 m/s mean ambient wind speed, respectively. These values were

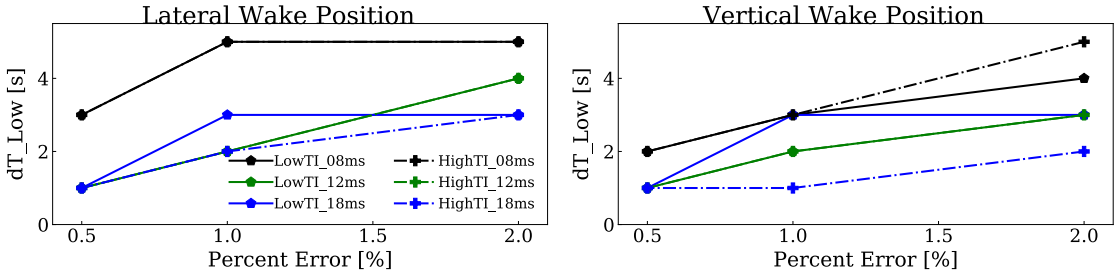

Figure 5. Required dT_{Low} value to ensure specified percent error is not exceeded.

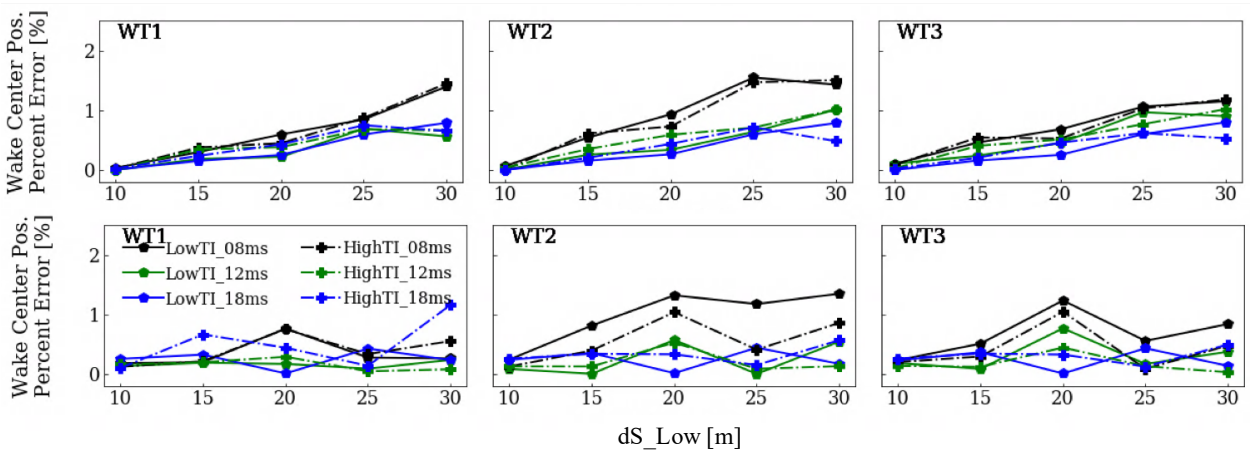

Figure 6. Percent error of lateral (top) and vertical (bottom) wake center position standard deviation associated with each dS_{Low} value at 8D downstream of each turbine.

driven primarily by the results for vertical wake meandering. These results closely match those estimated by Equation 1.

$$dT_{Low} \leq \frac{C_{meander} D_{wake}}{10 V_{hub}} \tag{1}$$

Here, $C_{meander}$ is a FAST.Farm input parameter for wake meandering (calibrated to be $C_{meander} = 1.9$ in [2]), D_{wake} is the wake diameter (which can be approximated by the rotor diameter), and V_{hub} is the mean wind speed at hub height. This equation is based on the low-pass cutoff frequency for wake meandering $\left(\frac{V_{hub}}{C_{meander} D_{wake}}\right)$ from [8] (in which $C_{meander} = 2$) and effectively specifies that at least 10 time steps at the highest frequency of wake meandering should be resolved.

3.1.2. Spatial Discretization Convergence plots of dS_{Low} for percent error of standard deviation of lateral and vertical meandering wake center position at 8D downstream of each turbine, relative to $dS_{Low} = 5$ m, are shown in Figure 6. As before, results are grouped by mean wind speed, though not as strongly as with dT_{Low} percent error, as shown in Figure 4. For dS_{Low}, the percent error does not exceed 3.5% for any turbine or downstream distance (or 2% at 8D, as shown in Figure 6). This indicates that there is little sensitivity to the spatial discretization of the low-resolution domain for the range of spatial discretizations considered. Nonetheless, the same process of identifying the maximum acceptable dT_{Low} for a given percent error limit was repeated for identifying the maximum required dS_{Low}, as shown in Figure 7. Again, a percent

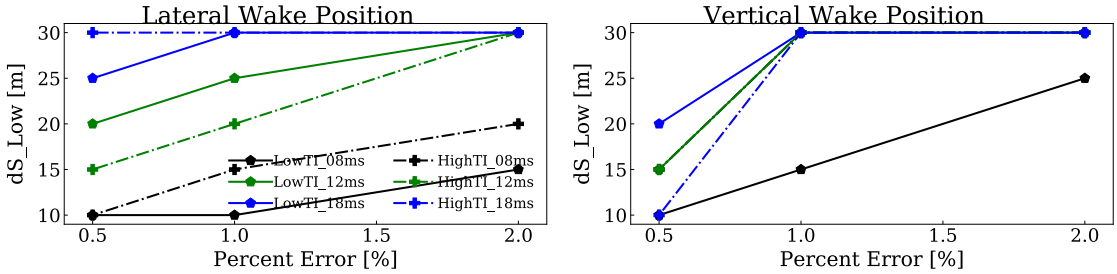

Figure 7. Required dS_{Low} value to ensure specified percent error is not exceeded.

error bound of 1% was chosen, resulting in selected dS_{Low} values to be 10, 20, and 30 m for 8, 12, and 18 m/s mean wind speed, respectively.

3.1.3. Summary Because the spatial and temporal discretization values are dependent on turbine rotor diameter, the derived temporal and spatial discretization values are summarized in Table 2 as functions of rotor diameter. These findings likely apply to all DWM-type models.

Table 2. Required discretization values in terms of rotor diameter (D, expressed in meters) to ensure percent error of standard deviation of meandering wake center position does not exceed 1%.

Freestream Velocity	dT_{Low} **[s]**	dS_{Low} **[m]**
8 m/s	$0.024D$	$0.079D$
12 m/s	$0.016D$	$0.16D$
18 m/s	$0.0079D$	$0.24D$

3.2. High-Resolution Discretization Study
The high-resolution wind domain is primarily responsible for ambient and waked inflow local to a turbine and, thus, turbine structural response and loads were the focus of the analysis. The detailed blade, drivetrain, and tower structural response from FAST.Farm has not yet been verified. This is considered acceptable for now, as this study assesses convergence based on a value as spatial and temporal resolution are refined. Specifically, convergence was assessed by comparing trends in the mean and standard deviation of various structural motions and loads, detailed in Table 3, for each turbine in the same manner as the low-resolution domain.

For all quantities in each case, the percent error was computed relative to the lowest discretization values considered – $dT_{High} = 0.05$ s for the temporal discretization study and $dS_{High} = 5$ m for the spatial discretization study. As with the low-resolution study, only the standard deviation of structural response was considered because the mean load values did not respond to changes in spatial and temporal discretization of the high-resolution domain. Additionally, results are grouped by load of interest, i.e., blade-root moment results report the lowest discretization level required over the three considered components.

Table 3. Structural motions and loads considered in the high-resolution discretization study.

Quantity of Interest	Component		
Blade-tip deflection	Out-of-plane	In-plane	
Tower-top deflection	Fore/aft		
Blade-root moments	Out-of-plane bending	In-plane bending	Pitching moment
Low-speed shaft moments at main bearing	0° bending	90° bending	Rotor torque
Tower-top moments	Fore/aft bending	Side/side bending	Yaw moment
Tower-base moments	Fore/aft bending	Side/side bending	Yaw moment
Generator power			

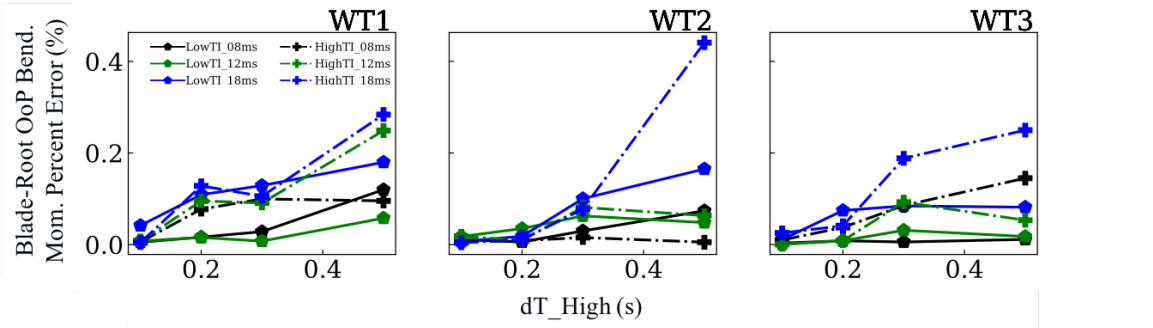

Figure 8. Percent error of blade-root out-of-plane bending moment standard deviation associated with each dT_{High} value of each turbine.

3.2.1. Temporal Discretization Convergence plots of dT_{High} for percent error of standard deviation of blade-root out-of-plane (OoP) bending moment of each turbine, relative to $dT_{High} = 0.05$ seconds, are shown in Figure 8. Overall, percent error converges to low values for decreasing dT_{High}. In general, there is no clear distinction between wind speed and TI. From these results, the maximum dT_{High} value acceptable for a desired percent error bound was selected for each inflow condition, considering each turbine and structural component, as shown in Figure 9. Required discretization levels vary depending on the quantity of interest. Thus, it is important to decide what structural components will be considered when selecting a high-resolution discretization level. Most notably, tower-base moments are the most sensitive to dT_{High}, whereas blade deflections and moments show no dependence on this value. Therefore, dT_{High} should be selected based on the highest frequencies influencing the excitation and response of the pertinent structural components. This is a frequently used rule of thumb, which is shown to be accurate in this work. This finding likely applies to all aeroelastic simulations.

To ensure accuracy of all structural components for the remaining study, the results from Figure 9 were concatenated to determine the maximum dT_{High} acceptable for a desired percent error bound considering all structural components. These required values are shown in Figure 10. As with the low-resolution domain, a percent error bound of 1% was chosen. Thus, for the subsequent discretization studies, dT_{High} was selected to be 0.1 seconds (corresponding to a Nyquist frequency cutoff of 5 Hz) for all ambient wind speeds. Most influential natural frequencies of the NREL 5-MW baseline turbine are less than 5 Hz, and the excitation associated with the rotational sampling of turbulence decreases with increasing frequency.

3.2.2. Spatial Discretization Convergence plots of dS_{High} for percent error of standard deviation of blade-root OoP bending moment of each turbine, relative to $dS_{High} = 5$ m, are

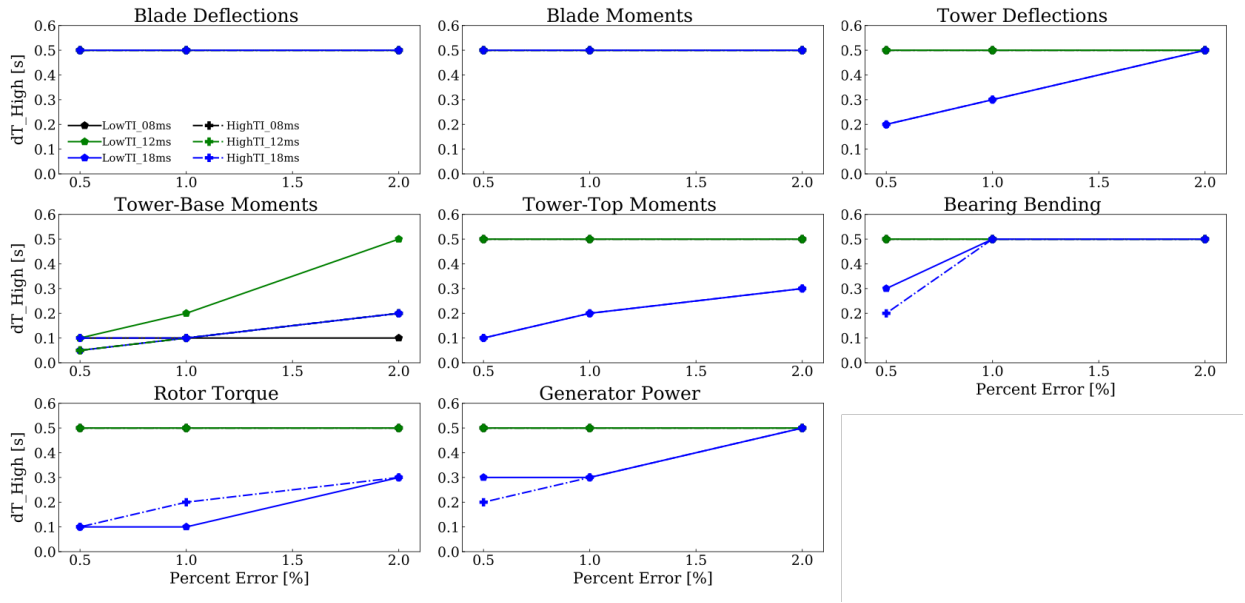

Figure 9. Required dT_{High} value to ensure specified percent error is not exceeded for each quantity of interest.

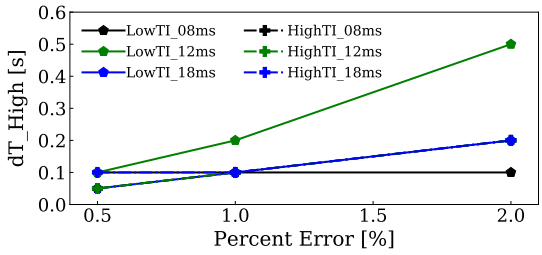

Figure 10. Required dT_{High} value to ensure specified percent error is not exceeded for all structural components.

shown in Figure 11. Overall, structural response is more sensitive to these ranges of dS_{High} than dT_{High}, but percent error still converges to a low percentage for decreasing dS_{High}. To understand why the standard deviations change with spatial discretization, power spectral density plots (PSDs) for the different discretization levels are plotted in Figure 12 for the high TI, 8 m/s inflow case. Shown in this plot is dependence of spectra content on the spatial discretization level. Specifically, a lower dS_{High} value results in higher spectral content and therefore an increased standard deviation. This is shown for both the high-frequency (top) and low-frequency (bottom) ranges, although the varied spectral content at the once-per-revolution frequency (about 0.15 HZ at this wind speed) is likely the most significant. From these results, the maximum dS_{High} value required for a desired percent error bound was selected for each inflow condition, considering each turbine and structural component. These required values are shown in Figure 13 for each load of interest. As was observed in the dT_{High} results, required discretization level changes based on which structural components are of interest. When all structural components are considered, $dT_{High} = 5$ m should be selected to ensure percent errors remain within 1%. This value also approximately corresponds to the maximum chord value of the NREL 5-MW turbine. Selecting a dS_{High} equivalent to this value has long been a rule of

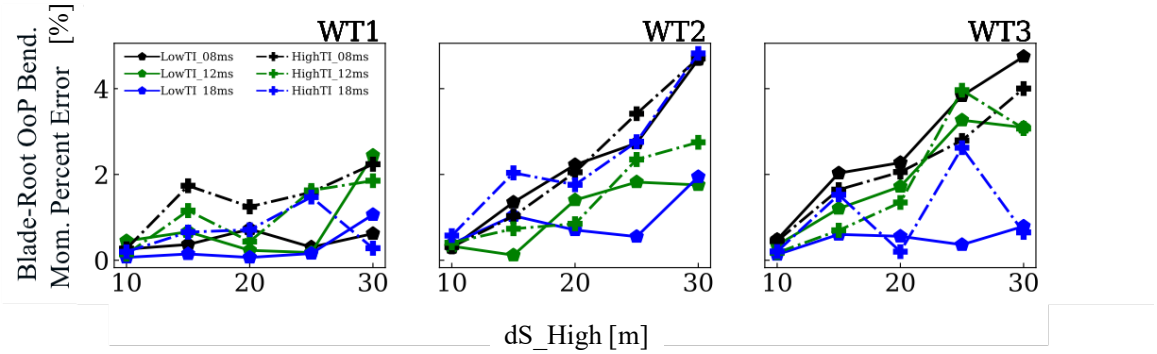

Figure 11. Percent error of blade-root out-of-plane bending moment standard deviation associated with each dS_{High} value of each turbine.

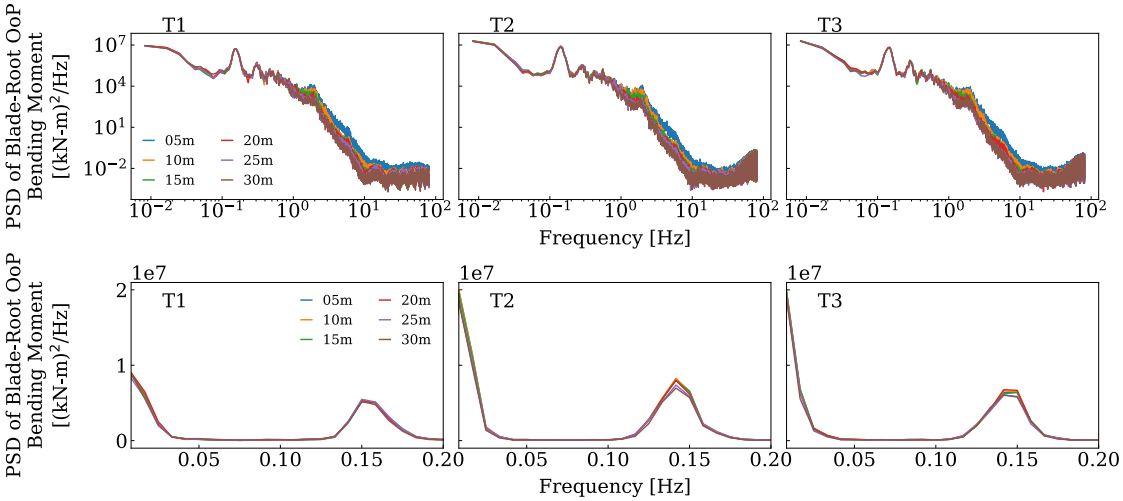

Figure 12. PSD of blade-root out-of-plane bending moment associated with each dS_{High} value of each turbine at high TI, 8 m/s inflow. Results are shown for all frequencies on a log-log scale (top) and focusing on a lower frequency range on a linear scale (bottom).

thumb and is confirmed in this work. This guidelines likely applies to all aeroelastic codes.

4. Conclusions and Discussion

Spatial and temporal discretization studies of the low-resolution and high-resolution domains have been completed. Convergence of low-resolution discretization was studied using percent error of the meandering wake center position standard deviation for a range of dT_{Low} and dS_{Low} values. For the NREL 5-MW reference turbine, temporal discretization levels were chosen that ensured percent error of wake center position standard deviation remain below 1% are 3, 2, and 1 s and spatial discretization levels are 10, 20, and 30 m for 8, 12, and 18 m/s mean ambient wind speed, respectively. When normalized by the rotor diameter, these guidelines are likely applicable to any dynamic wake meandering model. Convergence of high-resolution discretization was studied using standard deviation percent error of 16 structural outputs for a range of dT_{High} and dS_{High} values. Percent error values were found to be less dependent on mean ambient wind speed than the low-resolution domain. To ensure a percent error of $\leq 1\%$

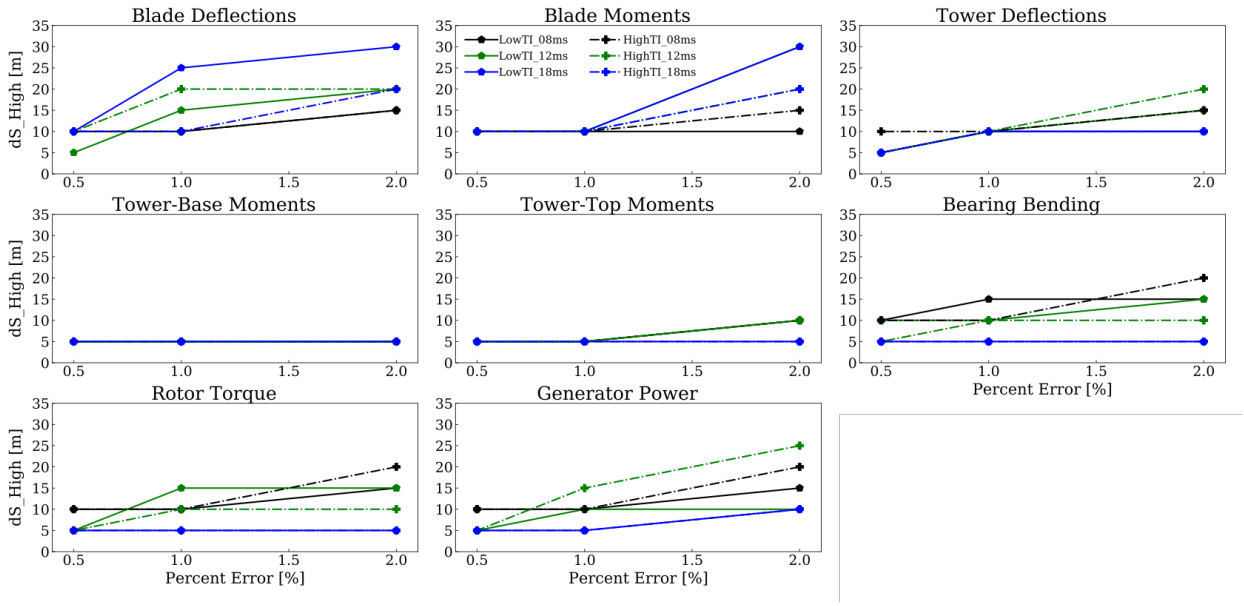

Figure 13. Required dS_{High} value to ensure specified percent error is not exceeded.

in standard deviation of all considered structural response outputs, a high-resolution time step that captures the highest excitation and natural frequencies in the system and a high-resolution spatial discretization comparable to the maximum airfoil cord length is recommended (0.1 s and 5 m for the NREL 5-MW turbine). These guidelines are likely applicable to any aeroelastic analysis.

Acknowledgments

This work was authored by the National Renewable Energy Laboratory, operated by Alliance for Sustainable Energy, LLC, for the U.S. Department of Energy (DOE) under Contract No. DE-AC36-08GO28308. Funding provided by the U.S. Department of Energy Office of Energy Efficiency and Renewable Energy Wind Energy Technologies Office. The views expressed in the article do not necessarily represent the views of the DOE or the U.S. Government. The U.S. Government retains and the publisher, by accepting the article for publication, acknowledges that the U.S. Government retains a nonexclusive, paid-up, irrevocable, worldwide license to publish or reproduce the published form of this work, or allow others to do so, for U.S. Government purposes.

References

[1] IEC 61400-1. Wind turbines - part 1: Design requirements. Technical Report 3rd edition, International Electrotechnical Commission, Geneva, Switzerland, March 2006.

[2] P. Doubrawa, J. Annoni, J. Jonkman, and et al. Optimization-based calibration of fast.farm parameters against sowfa. In *AIAA SciTech Forum*, 36th Wind Energy Symposium, Kissimmee, FL, January 2018. AIAA.

[3] B. Jonkman. Turbsim user's guide v2.00.00. Technical Report NREL/TP-xxxx-xxxxx, National Renewable Energy Laboratory, Golden, CO, October 2014.

[4] J. Jonkman, J. Annoni, G. Hayman, B. Jonkman, and A. purkayastha. Development of fast.farm: A new multiphysics engineering tool for wind-farm design and analysis. In *AIAA SciTech Forum*, 35th Wind Energy Symposium, Grapevine, TX, January 2017. AIAA.

[5] J. Jonkman, S. Butterfield, W. Musial, and G. Scott. Definition of a 5-mw reference wind turbine for offshore system development. Technical Report NREL/TP-500-38060, National Renewable Energy Laboratory, Golden, CO, February 2009.

[6] J. Jonkman, P. Doubrawa, N. Hamilton, and et al. Validation of fast.farm against large-eddy simulations. TORQUE 2018, Milano, Italy, June 2018. EAWE.
[7] J. M. Jonkman. Fast.farm user's guide and theory manual. Technical Report NREL/TP-xxxx-xxxxx, National Renewable Energy Laboratory, Golden, CO, Unpublished 2018.
[8] G. C. Larsen, H. A. Madsen, K. Thomsen, and et al. Wake meander: A pragmatic approach. *Wind Energy*, 11:337–95, 2008.
[9] K. Shaler, J. Jonkman, P. Doubrawa, and N. Hamilton. Fast.farm response of varying wind inflow techniques. In *AIAA SciTech Forum*, 37th Wind Energy Symposium, San Diego, CA, January 2019. AIAA.